J. Automation & Systems Engineering 7-3 (2013): 105-114

JASE
Journal of Automation & Systems Engineering

SCIM Diagnosis Using 3-D Plot CWT

S. Bourdim and K. E. Hemses

Abstract- In this paper, a new results in induction motor diagnosis approach for identifying rotor broken bar/end-ring failures is presented, the approach is based on the analysis of the stator current in steady state, using the Windowed Fourier transform analysis and comparison between Continuous Wavelet Transform (CWT) in 2-D time-frequency plot and 3-D time frequency plot respectively Using the simplified dynamic model of the squirrel cage induction motor; Simulation results are reported to validate the effectiveness of the wavelet transform and its ability to provide a local representation of the non stationarity current signal particularly in 3-D time frequency plot and to overcome the limitation of the classical approaches based on Fourier Analysis .

Keywords: Fault diagnosis, broken rotor bar/end-ring , Fourier analysis, induction machine, Motor Current Signature Analysis, 2-D and 3-D plot continuous wavelet transform.

NOMENCLATURE

CWT: Continuous Wavelet Transform.

DWT: Discrete Wavelet Transform.

FFT: Fast Fourier Transform

MCSA: Motor Current Signature Analysis.

STFT: Short Time Fourier Transform.

SCIM: Squirrel Cage Induction Machine.

db40: Daubechies family 40.

2-D plot: Two dimensions plot.

3-D plot: Three dimensions plot.

1. INTRODUCTION

CONDITION MONITORING and fault diagnosis of induction machines is enormously important in any industrial setup, due to the reliability and low cost of this machines which are widely used in industrial applications [1],[2].Among all the induction faults, almost 10% of them are caused by rotor broken bar/end ring [3]. Generally, the diagnosis of induction machine faults is carried out by means of Motor Current Signature Analysis (MCSA), which has been proven to be suitable in wide range of applications and by applying the fast Fourier transform to the steady state current; in case of broken bars, current spectrum for a motor shows the presence of characteristic harmonic whose

S. Bourdim is with LEB (Electrotechnic Laboratory Batna), Department of Electrical Engineering- Hadj Lakhdar Batna University: Av. El hadj Boukhlouf, Batna 05000 Algeria (e-mail: samiahakima@yahoo.fr).

K. E. Hemses is with LAS (Automatic Laboratory Sétif), Department of Electrical Engineering, Ferhat Abbas Sétif University, Algeria (e-mail: hemses.kamel@gmail.com).

frequencies are given by (1) Where s is the slip, p is the number of poles pairs and f_s is the supply frequency $(k \in N, k/p = 1,3,5....)$ [1].

$$f_{bb} = f_s(1 \pm 2sk) \tag{1}$$

Taking $k = 1$ in (1), the frequencies of the lower and upper sideband harmonics (LSH and USH) are obtained; these harmonics are the basis of the diagnostic in the conventional MCSA approach [4].

In healthy conditions only the fundamental frequency f_s exists in stator currents by a single clear peak. Some experimental results show that we can find right and left sideband in healthy machine spectrum because its construction asymmetry, but these components are with small magnitude compared with a faulty machine [5].

If the rotor part is damaged the rotor symmetry of the machine is lost and the frequencies of the sideband amplitude are small, and by increasing the number of broken bars, amplitudes of harmonics $f_s(1 \pm 2s)$ and $f_s(1 \pm 4s)$ increase considerably. In addition, frequency components due to the fault are closer to the fundamental frequency and become smaller as the slip gets smaller values. Thus, it is much more difficult to identify them in low load operation and even harder in the case of just one broken bar or end-ring fault. To compensate this phenomenon, a window, a time-domain weighting function, is commonly adapted to reduce this drawback [5]. Window forces the amplitude of the sampled signal to zero at both ends of the time record. Selection of a proper window can prevent spectral leakage, smearing of energy across the frequency spectrum caused by the transformation of signals that are not periodic within the time record [5].

By windowing technique (Short Time Fourier Transform) STFT, it is possible to detect the sideband harmonics and to evaluate their magnitudes and their frequencies much more accurately. The choice of the window has a very important role at the time of the frequency analysis. The window must have a signal containing the more information in order to make it capable of defects diagnosis [5]. the major inconvenience of this method is that the length of the window is fixed, so there is no information about local variation of a signal at certain frequency during a particular short period of time, Also, capturing such a signature may necessitate a high sampling rate that may not be acceptable to sample the signal for a long period of time; a flexible sampling scheme is desirable. For the reasons to be shown next, wavelet transform is more suitable in such a case. It can employ a long window and low sampling rate for a low-frequency component in the signal, and at the same time a short window and high sampling rate for a high-frequency component. Additionally, wavelet transform exhibits time frequency localisation, which gives a more precise description of the signal, providing more informative data for condition monitoring [6].

There are two kinds of wavelet transform, namely, continuous wavelet transforms (CWT) and discrete wavelet transform (DWT). CWT is defined as the sum over all time of the signal multiplied by scaled, shifted versions of the wavelet function. Discrete wavelet transform (DWT) has been defined to analyze the signals with a smaller set of scales and specific number of translations at each scale [5].

The major works of diagnostic of induction machine with CWT are in 2-D time-frequency plot like in [4], [7], [8].

The main aim of this paper is to present a new method for the diagnosis of broken rotor

bars and broken end-ring in 3-D time frequency plot of CWT for the analysis of the stator current in steady state operation and show their clarity comparing with 2-D plot of CWT, as a result overcome the averaging problems of classical FFT and STFT method.

This paper is organized as follows. Section II presents a theoretical background for the wavelet transform in its two variants CWT and DWT, some detail of our phraseology work are presented In the beginning of section III and simulation results for rotor broken bars/end ring fault analysis in steady state are presented and commented. Conclusions and perspectives are given in section IV. Finally we finish our article by appendix and sufficiently wealthy reference.

2. WAVELET TRANSFORMS

It is required to use time-frequency basis functions with different time supports to analyze signal structures of different sizes. The wavelet transform is relatively new mathematical technique, an extension of the Fourier transform, projects the original signal down onto wavelet basis functions and provides a mapping from the time domain to the time scale plan. In recent years wavelet analysis has been applied to many areas of signal processing. The way wavelet analysis localize signal's information in the time-frequency plane (time-scale would be a more appropriate term) makes it especially suitable for the analysis of non-stationary signals and a good alternative to traditional STFT analysis.[9]. So the wavelets transform in its two kinds, CWT and DWT plays a very important role in signal processing, we start by the CWT witch our aim work.

2.1. CONTINUOUS WAVELET TRANSFORM

The continuous wavelet transform (CWT) was developed as an alternative approach to the STFT to overcome its resolution problem. The wavelet analysis is done in a similar way to the STFT analysis, in the sense that the signal is multiplied with a function, with the wavelet, and the transform is computed separately for different segments of the time-domain signal.

The continuous wavelet transform is defined by the following equation:

$$CWT_x^{\psi}(\tau,s) = \Psi_x^{\psi}(\tau,s) = \frac{1}{\sqrt{|s|}} \int x(t)\, \psi^*\left(\frac{t-\tau}{s}\right) dt \tag{2}$$

As it can be seen the transformed signal is a function of two variables τ and s (the translation and scale parameters respectively) , $\psi(t)$ called the mother wavelet, a prototype for generating the other window function X . The term translation is used in the same sense as it was used in the STFT; it is related to the location of the window, This term, obviously, corresponds to time information in the transform domain, while scale is way of viewing the frequency content, high scales correspond to lower frequency meaning thereby better resolution, and low scales correspond to high frequency. The most efficient and compact form of the wavelet analysis is accomplished by the decomposing a signal into a subset of translated and dilated parent wavelets, where these various scales and shifts in the parent wavelet are related based on powers of two. Full representation of a signal can be achieved using a vector coefficients the same length as the original signal. [10], [11]

2.2. DISCRETE WAVELET TRANSFORM

For the discrete wavelet transform (DWT) the main idea is the same as it is in the case of CWT, but it is considerably easier and faster to implement. A time-scale representation of a

digital signal can be obtained using digital filtering techniques. Filters of different cutoff frequencies are used to analyze the signal at different scales. Multi-resolution analysis refers to the procedures to obtain low-pass approximations and high-pass details from the original signal. Approximations and details are obtained through a succession of convolution processes. The original signal is divided into different scales of resolution, rather than different frequencies, as in the case of Fourier analysis [12]. The algorithm of multi-resolution decomposition is given in Fig.1; three levels of decomposition are shown. The signal is passed through a series of high pass filters to analyze the high frequencies, and it is passed through a series of low pass filters to analyze the low frequencies .The maximum number of wavelet decomposition levels are determined by the length of the original signal and the level of detail required. With reference to Fig.1 [13], the multi-resolution procedures are defined as follows:

$$D_j(n) = \sum_k h(k)\, \mathrm{A}_{j-1}(n-k) \tag{3}$$

$$A_j(n) = \sum_k l(k)\, \mathrm{A}_{j-1}(n-k) \tag{4}$$

Where l and h are low-pass and high-pass filter vectors respectively, D_j and A_j are the detail and approximation at resolution $j = 1,2,.....,J$, respectively, A_{j-1} is the approximation of the level immediately above level $j, k = 1,2,.....,K$ where K is the length of the filter vector [8].

The original signal S is first passed through a half band high-pass filter H and a low-pass filter L, after the filtering, half of the samples can be eliminated according to the Nyquist's rule. Simply discarding every other sample will subsample the signal by two, and the signal will then have half the number of points.

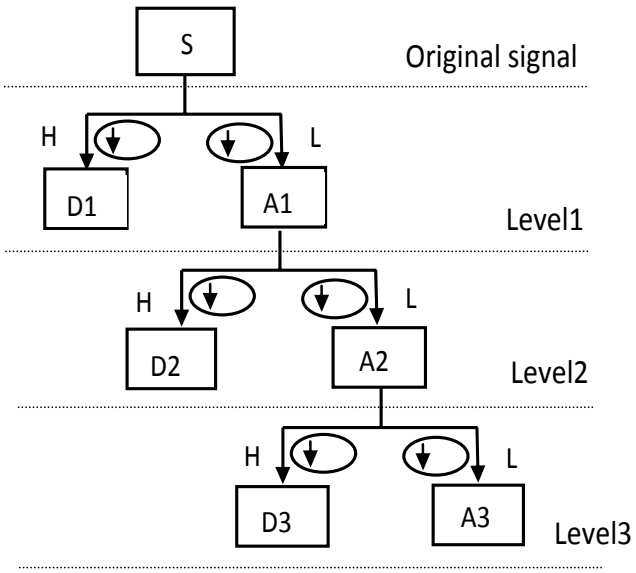

Fig. 1 Multi-resolution and wavelet decomposition

The scale of the signal is now doubled. Note that the filtering removes a part of the frequency information (changing the resolution of the signal), but leaves the scale unchanged. Only the subsampling process changes the scale. The above procedure constitutes one level of decomposition, and is also known as the subband coding. It can be repeated for further decomposition. At every level, the filtering and subsampling will result in half the number of samples (and hence half the time resolution) and half the frequency band spanned (and hence doubles the frequency resolution). This process can continue until two samples are left. The frequencies that are most prominent in the original signal will appear as high amplitudes in that region of the DWT signal that includes those particular frequencies. The difference of this transform from the Fourier transform is that the time localizations of these frequencies will not be lost. This procedure in effect offers a good time resolution at high frequencies, and good frequency resolution at low frequencies [14].

3. SIMULATION RESULTS

In order to test the efficiency of the wavelet transform, simulations results of the induction motor drive are obtained were carried out using the Matlab simulation package. The motor used in the simulation study is In order to test the efficiency of the wavelet transform, simulations results of the induction motor drive are obtained were carried out using the Matlab simulation package. The motor used in the simulation study is the Multi-Loop Model and parameters as the basis of this simulation, which is more convenient than the classical method for the analysis of inner faults. According to the model, an AC machine is considered as an electric circuit linked with ferromagnetic circuit. The difference between AC machines and general static circuits is the existence of relative movement between the stator and the rotor for the former. [15], [16].

It is a 450 W, 220 V, 50 Hz, 1-pole induction motor, with a rotor with 27 bars, for more detail about the simulation model the parameters machine found in the appendix (section VI).

Broken rotor bars can be detected by monitoring the stator current spectral components. These spectral components are illustrated by equation (1).

The amplitude of the left sideband is proportional to the number of broken bars, the spectral component associated with broken rotor bars is found at the frequency $f_s(1-2s)$.

Figure 2 in their cases (a, b, c, d, e, f) for healthy machine in case (a) and in faulty induction machine with different number of broken bars/end ring in cases (b ,c ,d ,e ,f) shows the windowed Fourier analysis of the stator current using a Hamming window.

As we see in case (a), it is clear that the only fundamental frequency f_s exists in stator currents by a single clear peak, the amplitude is highest in the frequency of 50 Hz.

The result analysis in the others cases are done for various broken bars condition such as 1, 2 and 3 broken bars.

In cases (b) and (c),figures indicate that amplitudes of the lower and upper side bands frequency components $(f_s(1\pm 2s))$, $(f_s(1\pm 4s))$ are clear than amplitudes in cases (d) and (e) were there is more than two broken bars. According to this analysis, we can said there is no different between cases (c two broken bars) and (d and e three broken bars) it means when the number of broken bars increase, amplitudes of harmonics $f_s(1\pm 4s)$ and $f_s(1\pm 6s)$ increase but there is not a linear trend.

If any fault is occurred then amplitude of the side lobes are increased that is clear indication of the fault. It is due to the reverse rotating magnetic field in the inductor and mutual inductance, in fault diagnosis procedure, the limitation of STFT are the lost of localisation in time domain, STFT would give erroneous results in this case and improved that is not effective for rotor broken bars detection, So the broken bar frequencies around the fundamental frequency are not clearly visualized.

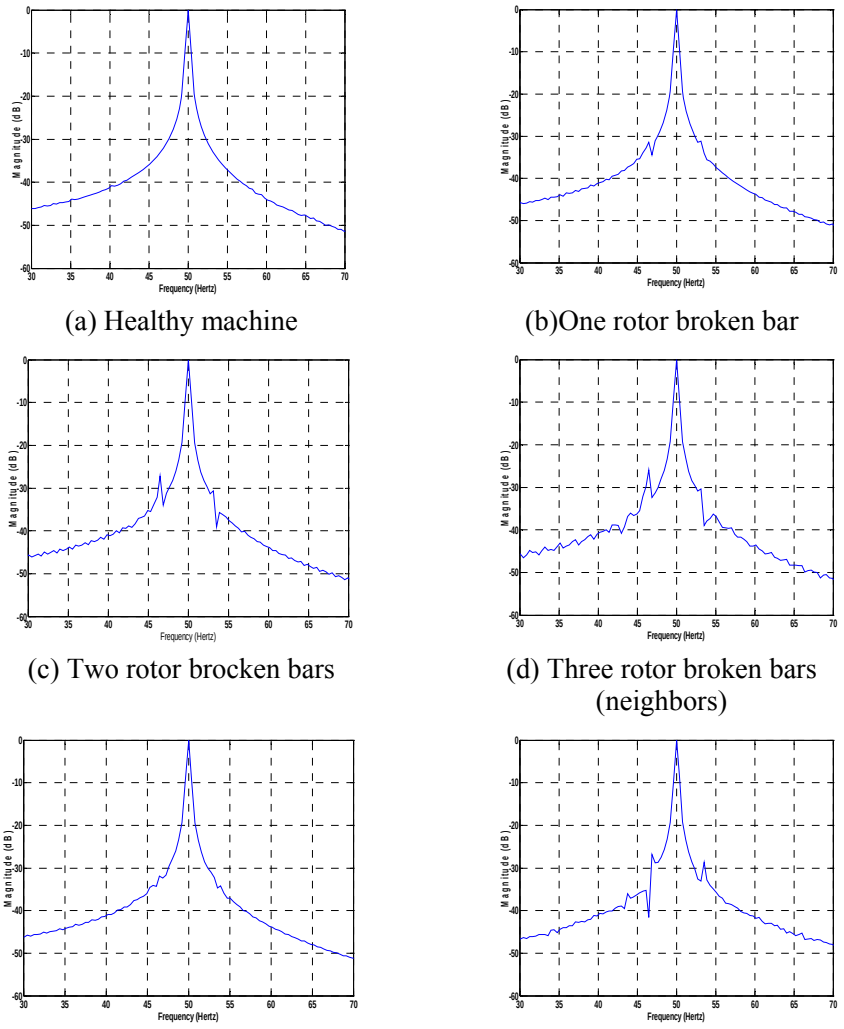

(a) Healthy machine (b)One rotor broken bar

(c) Two rotor brocken bars (d) Three rotor broken bars (neighbors)

(e) Three rotor broken bars (spaced symmetrically) (f) Rotor broken one of end ring

Fig. 2 STFT of the Current stator
(a)healthy machine, (b) with One rotor broken bar , (c) Two rotor brocken bars , (d) Three rotor broken bars(neighbors), (e) Three rotor broken bars (spaced symmetrically) and (f) Rotor broken one end ring

In recent years, the current signal was analyzed by more advanced signal processing technique, wavelet was used to extract suitable features related to faults, the rotor fault diagnosis using wavelet transform is widely used in these days, the simulation results obtained from the wavelet transform for rotor broken bars are as shown in figures (3, 4, 5, 6, 7) . The following figures give the CWT of the statorique current phase in 2-D and 3-D plot dimensions. The case (a) represents the healthy state the arrow show the beginning of steady state, at t=2 second we broke one bar, the result corresponding case (b) in fig.4 explain this fracture in 2-D plot and we note down the instance of failure by arrow.

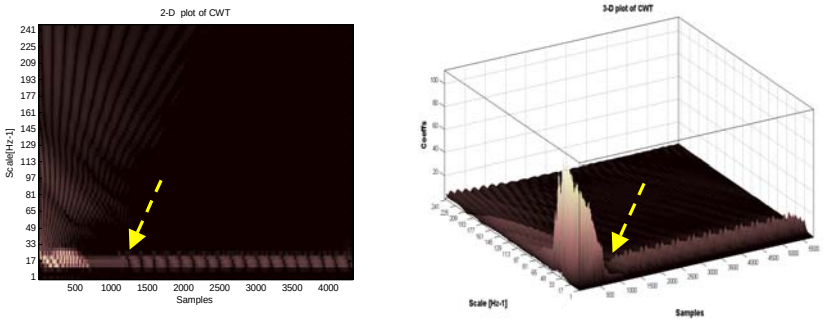

Case (a) with 2-D plot of CWT Case (a) with 3-D plot of CWT

Fig. 3 CWT of the Current stator healthy state

In 3-D plot this variation given by one convexity as follow in fig .4

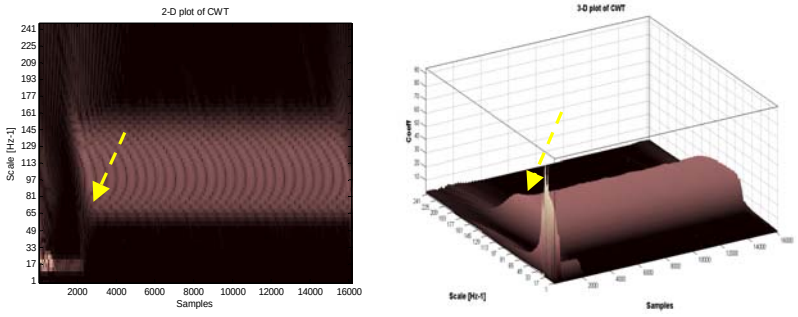

Case (b) with 2-D plot of CWT Case (b) with 3-D plot of CWT

Fig. 4 CWT of the Current stator with one rotor broken bar

In case (c) corresponding fig. 5, we observe two convexities corresponding the broken of two neighbours bars at t=2 second and t=3second respectively in 3-D plot and the same variation are demonstrated by two arrows in 2-D plot.

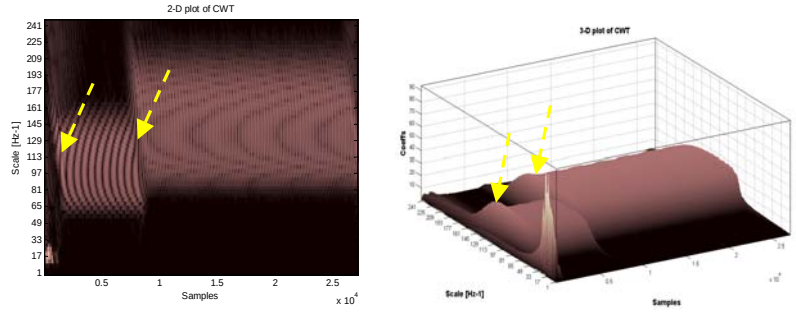

Case (c) with 2-D plot of CWT Case (c) with 3-D plot of CWT

Fig .5 CWT of the Current stator with two rotor broken bars

The results are very clear in fig.6 when we observe the broken of three neighbours bars: case (d) and three broken bars spaced symmetrically in case (e)

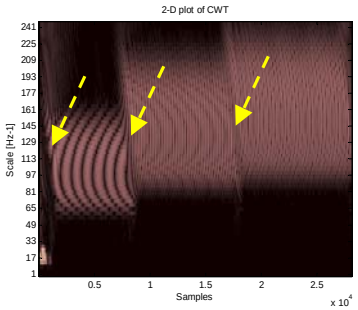

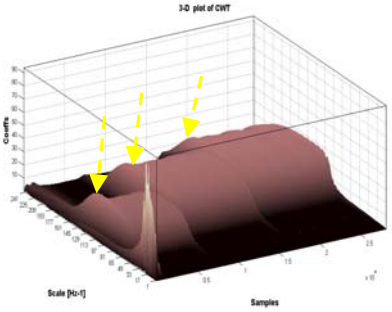

Case (d) with 2-D plot of CWT Case (d) with 3-D plot of CWT

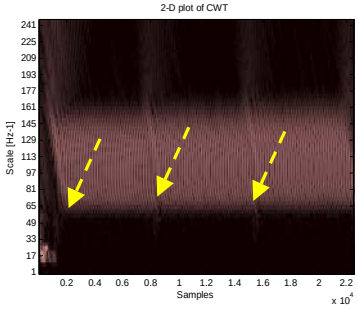

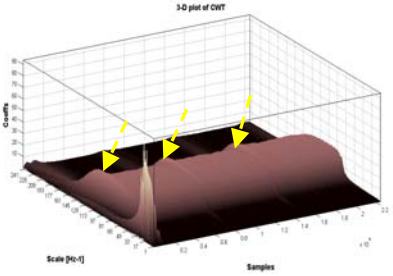

Case (e) with 2-D plot of CWT Case (e) with 3-D plot of CWT

Fig. 6 CWT of the Current stator bars ,(d) Three rotor broken bars (neighbors), (e) Three rotor broken bars (spaced symmetrically)

Finally the case (f) corresponding the broken of one end rings. According to Figures (3, 4, 5, 7, 8) we notice that the figures of the CWT gives the variations which cross in the time (NB: for healthy machine 4 second corresponding 4329 samples) that is the time of the break of the bar is made. Thus from these results can say that CWT localizes well the defect we also notice that we have a weakening system the interval of simulation is increase with the increase of number of broken bars.

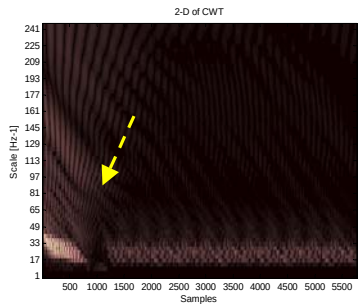

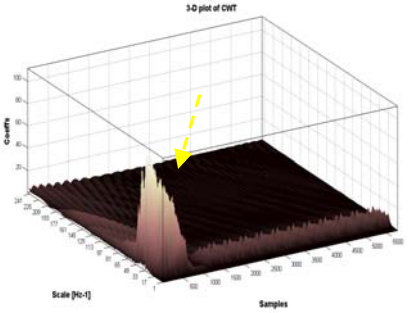

Case (f) with 2-D plot of CWT Case (f) with 3-D plot of CWT

Fig. 7 CWT of the Current stator with Rotor broken one end ring

4. CONCLUSION

Finally it can be concluded that the wavelet analysis of the measured line current can be used successfully for the rotor fault detection of wound rotor induction machines. In further works the above-described method will be extended also to the rotor fault detection of the squirrel cage induction machine (SCIM), and also for the diagnosis of the all the other

faults that can be detected by the motor current signature analysis (rotor eccentricity, etc.). Also other wavelet transform methods (for example the continuous wavelet transform) will be studied to be applied in electrical machines fault diagnosis.

5. APPENDIX

Parameters of induction motor used in simulation

Output power	P= 450 w
Stator voltage	V= 127 v
Stator frequency	f = 50 Hz
Pole Number	P= 1
Number of rotor bars	Nr= 27
Stator resistance	Rs = 4.1Ω
Stator inductance	Lsf = 17.5
Rotor bar resistance	Rb=74 μΩ
End ring inductance	Le= 0.33 μH
Number of turns per	Ns=193
Ring resistance	Re= 74 μΩ
Rotor bar inductance	Lb= 0.33 μH
inertia Moment	J= 4.5 10-3
Constant	k0=5.10-6

6. REFERENCES

[1] I. P. Georgakopoulos, E. D. Mitronikas, and A. N. Safacas " Detection of Induction Motor Faults in Inverter Drives Using Inverter Input Current Analysis", IEEE Transactions on industrial electronics, Vol. 58, N^{O} 9, pp 4365-4373, September 2011.

[2] H. Abu-Rub, A. Iqbal, S. M. Ahmed, J. Guzinski, M. Adamowicz, M. Rahiminia "Rotor Broken Bar Diagnostics in Induction Motor Drive Using Wavelet Packet Transform and ANFIS Classification", IEEE International Electric Machines & Drives Conference (IEMDC), pp 365 -370 , 2011.

[3] W. Li, W. Xuan, W. Dongxu "On-line Rotor Fault Detection In Squirrel Cage Induction Motors Based On Wavelet Analysis", IEEE Chinese Control and Decision Conference, pp 3854-3856, 2010.

[4] J. P. Llinares, J. A. Antonino-Daviu, M. R.Guasp, M. P.Sanchez, and V. C. Alarcon "Induction Motor Diagnosis Based on a Transient Current Analytic Wavelet Transform via Frequency B-Splines" IEEE Transactions on Industrial Electronics, pp 1530 - 1531 Vol. 58, N^{O}.5, MAY 2011.

[5] N. Mariun, M. R. Mehrjou, M. H. Marhaban, N. Misron "An Experimental Study of Induction Motor Current Signature Analysis Techniques for Incipient Broken Rotor Bar Detection" Proceedings of the International Conference on Power Engineering, Energy and Electrical Drives Torremolinos (Málaga), Spain. May 2011.pp 1-5, 2011.

[6] P. Tavner, L. Ran, J. Penman and H. Sedding "Condition monitoring and rotating electrical machines", Power and energy series, Vol. 56, Printed in the UK by Athenaeum Press Ltd, Gateshead, Tyne & Wear, ISBN 978-0-86341-739-9, .P.122,. 2008.

[7] M.P.Sanchez, M. Riera-Guasp, Jose A. Antonino-Daviu, J. Roger-Folch, J. Perez-Cruz, and R. Puche-Panadero "Diagnosis of Induction Motor Faults in the Fractional Fourier Domain " IEEE Transactions on Instrumentation and Measurement, Vol. 59, no. 8, August 2010

[8] A. Bouzida, O. Touhami, R. Ibtiouen, A. Belouchrani, M. Fadel, A.Rezzoug "Fault Diagnosis in Industrial Induction Machines through Discrete Wavelet Transform",, IEEE Transactions on Industrial Electronics Vol. 58, pp 4385 – 4395 , Sep 2011 .

[9] T. W. S. Chow, S. Hai "Induction Machine Fault Diagnostic Analysis With wavelet Technique" IEEE Transaction on Industrial Electronics, Vol. 51, N^{O}. 3, pp 558-565, June 2004.

[1]0 A. Menacer, R. Kechida, G. Champenois, S. Tnani "Application of the Fourier and the Wavelet Transform for the Fault Detection in Induction Motors at the Startup Electromagnetic Torque", IEEE International Symposium on Power Electronics & Drives (SDEMPED), pp 664-668. 2011.

[11] W.Yang, P. J. Tavner, M.Wilkinson," Wind Turbine Condition Monitoring and Fault Diagnosis Using both Mechanical and Electrical Signatures" Proceedings of the 2008 IEEE/ASME International Conference on Advanced Intelligent Mechatronics July 2 - 5, 2008, Xi'an, China

[12] C. H. Kim , R. Aggarwal, "Wavelet transforms in power systems", Power Engineering Journal, August 2001, pp. 193-202. 2001.

[13] R. Khan, M. Al-Dabbagh. "Decomposition of power systems harmonics using wavelet technique", Electrical Energy and Control Systems 2008.

[14] K. Li, P. Chen, and H.Wang ,"Intelligent Diagnosis Method for Rotating Machinery Using Wavelet Transform and Ant Colony Optimization" IEEE Sensors Journal, Vol. 12, no. 7, July 2012

[15] S. Bourdim**,** "méthode ondelettes et Bayesienne pour le diagnostic: Application aux machines électriques"**,** Magister dissertation, directed by Dr. K. E. Hemsas, Electrotechnics Dept., UFAS, Setif, Algeria, 2011.

[16] J. Gao, L. Zhang, X. Wang, "AC Machine Systems: Mathematical Model and Parameters, Analysis, and System Performance", ISBN 978-7-302-19342-5, Tsinghua University Press, Beijing, chapter one pp 1- 2, chapter six, pp415-431, 2009.